Carbon-nanotube-supported POXA1b laccase and its hydrophobin chimera for oxygen reduction and picomolar phenol biosensing

Ilaria Sorrentino, Ilaria Stanzione, Alessandra Piscitelli, Paola Giardina, Alan Le Goff

8 (2021) 100074

Contents lists available at ScienceDirect

Biosensors and Bioelectronics: X

journal homepage: www.journals.elsevier.com/biosensors-and-bioelectronics-x

Carbon-nanotube-supported POXA1b laccase and its hydrophobin chimera for oxygen reduction and picomolar phenol biosensing

Ilaria Sorrentino [a], Ilaria Stanzione [b], Alessandra Piscitelli [b], Paola Giardina [b,*], Alan Le Goff [a,*]

[a] Department of Molecular Chemistry, University Grenoble Alpes, CNRS, 38000, Grenoble, France
[b] Department of Chemical Sciences, University Federico II, 80126, Naples, Italy

ARTICLE INFO

Keywords:
Laccase
Hydrophobin
Carbon nanotubes
Catechol
Dopamine
Biosensing

ABSTRACT

The immobilization of POXA1b laccase and its hydrophobin-fused chimera was performed at pristine Multi-walled Carbon Nanotube (MWCNT) and MWCNT-modified electrodes by electrografting of a 2-diazoniumanthraquinone salt. The influence of the hydrophobin domain and the MWCNT functionalization with anthraquinone groups towards immobilization of laccase was compared by direct electrochemistry under O_2 and electrochemical biosensing of phenols. The hydrophobin domain affords the stable dispersion of MWCNT in water/ethanol, while being detrimental to the direct electron transfer between POXA1b and the electrode. On the contrary, the stronger hydrophobic interactions between anthraquinone and laccase affords direct electrochemistry of POXA1b and enabled the design of a highly sensitive phenol biosensor, reaching a limit-of-detection (LOD) of 2 pM and sensitivity of 23,600 mA L mmol^{-1} cm^{-2} for catechol, and a LOD of 15 nM and sensitivity of 0.053 mA L mmol^{-1} cm^{-2} for dopamine.

1. Introduction

The use of nanostructured carbons such as carbon nanotubes (CNTs) or graphene have tremendously improved the performance of biosensors (Holzinger et al., 2017; Sotiropoulou et al., 2003; Valentini et al., 2013). In particular, the nanowire morphology of CNTs, coupled with excellent conductivity and biocompatibility, have made CNTs a material of choice for biosensor electrodes (Holzinger et al., 2017). CNT electrode films exhibit high electroactive area and can be easily modified by many types of reactions to attach biomolecules (Le Goff and Holzinger, 2018). Their thin nanowire morphology can also make them excellent candidates for closely approaching the catalytic pocket and activating direct electron transfer (DET) with many enzymes, even those possessing deeply embedded active sites.

Laccases (*p*-diphenol-dioxygenoxidoreductases; EC 1.10.3.2) are multicopper oxidases involved in the catalysis of the oxidation of a wide range of aromatic substrates using oxygen as a co-substrate and water as the only by-product. These metalloenzymes are envisioned as renewable biocatalysts in many applications such as bioremediation, organic synthesis, biobleaching, biofuel cells and biosensing (Le Goff et al., 2015; Mano and de Poulpiquet, 2017; Pezzella et al., 2015). Among the laccase family, POXA1b from *Pleurotus ostreatus* has peculiar characteristics such as its stability and activity over a wide range of pHs and temperatures, as well as its high redox potential (Pezzella et al., 2017). Recently, we demonstrated that the class I hydrophobin Vmh2 from the same fungus *P. ostreatus*, was able to disperse graphene by ultrasonic wave exfoliation from graphite (Gravagnuolo et al., 2015). Hydrophobins strongly interact with several hydrophobic surfaces such as Teflon (Askolin et al., 2006; Portaccio et al., 2015; White, 2004), polystyrene (Wang et al., 2010), silicon (De Stefano et al, 2007, 2009), steel (Longobardi et al., 2015), and graphene (Gravagnuolo et al., 2015). This appealing ability has been further extended to laccases by genetic fusion of the hydrophobin to POXA1b(Sorrentino et al., 2019a,b), allowing achievement of simple and stable immobilization of the enzyme on different surfaces such as polystyrene or graphene sheets (Sorrentino et al, 2019, 2020). These biofunctionalized surfaces were then employed in the design of laccase-based phenol biosensors(Sorrentino et al., 2020).

The main objective of this work was to study the interaction of both POXA1b and its hydrophobin-fused chimera, POXA1b-Vmh2, with Multi-Walled CNT (MWCNT) sidewalls. MWCNTs were modified using diazonium electrografting in order to introduce anthraquinone groups which are known to increase the hydrophobicity of the electrode surface and interact with the substrate pocket of laccases (Bourourou et al., 2013; Sorrentino et al., 2019a,b; Sosna et al., 2012). Herein, we

* Corresponding authors.
E-mail addresses: giardina@unina.it (P. Giardina), alan.le-goff@univ-grenoble-alpes.fr (A.L. Goff).

https://doi.org/10.1016/j.biosx.2021.100074
Received 28 January 2021; Received in revised form 11 May 2021; Accepted 2 June 2021
Available online 20 June 2021

investigated for the first time the influence of anthraquinone-modified MWCNTs on the immobilization of POXA1b and POXA1b-Vmh2. In addition, direct electrochemistry in the presence of O_2 was explored as well as electroenzymatic oxidation of catechol and dopamine by these bioelectrodes.

2. Materials and methods

2.1. General procedure

Multi-Walled Carbon Nanotube (MWCNTs, > 99% purity) and all other reagents were purchased from Sigma-Aldrich (Saint Louis, Missouri, USA) and were used without further purification. All chemicals employed in this work were of analytical grade. All solutions were prepared with Milli-Q deionised water (18.2 MΩ cm−1). Freshly prepared solutions were used in all experiments by diluting the corresponding standard stock solution.

The electrochemical experiments were performed with a conventional three-electrode electrochemical cell using either a Biologic VMP3 Multi Potentiostat or Ametek Multipotentiostat Princeton Applied Research (Wokingham, UK). MWCNT bioelectrodes were used as working electrodes, with a saturated calomel (SCE) and a platinum (Pt) wire acting as the reference and counter electrode, respectively. All experiments were conducted at room temperature. All simulated curves were obtained via Origin Pro 9.0. Error bars were estimated from three measurements recorded per sample.

2.2. Preparation of the glassy carbon-modified MWCNT electrode

The working electrodes were modified glassy carbon electrodes (3 mm diameter). 5 mg mL^{-1} N-Methylpyrrolidone (NMP) dispersions of MWCNTs (purity > 99% Sigma-Aldrich) were prepared by 30 min in an ultrasonic bath (Fisher scientific FB 15050) until a homogeneous black suspension was obtained. Then 20 μL of the MWCNTs solution was drop-casted on a glassy carbon electrode (GCE) and NMP was removed under vacuum to obtain a 5-μm-thick film. Then, these MWCNT-coated glassy carbons electrodes were modified by electrografting in a 2 mM 2-diazoniumanthraquinone tetrafluoroborate solution in 0.1 tetrabutylammonium perchlorate (TBAP)/MeCN according to previously-described procedures(Sorrentino et al., 2019a,b). After incubation, the electrodes were washed with MeCN and water.

2.3. Laccase enzyme

Both wild-type enzyme POXA1b and fusion protein POXA1b-Vmh2 were produced as recombinant proteins by the yeast *Pichia pastoris* and secreted in the culture media. The supernatant, following centrifugation for 15 min at 6000 rpm at 4 °C, was concentrated and dialyzed against 50 mM Tris-HCl buffer, pH 8.0, using Centricon Centrifugal Filter Units 10 kDa (Sartorius Vivaspin®). The enzymes were used without additional purification steps.

The laccase activity was assayed by monitoring at 420 nm ($\varepsilon_{420\ nm} = 3.6 \times 10^{4}\ M^{-1}\ cm^{-1}$) the oxidation of ABTS (2,2′-azino-bis (3-ethylbenzothiazoline-6-sulphonic acid)) at room temperature: the assay solution contained 2 mM ABTS and 50 mM phosphate/citrate buffer, pH 3.0.

2.4. Immobilization of laccase enzymes

The modified MWCNT electrodes were incubated with 20 μL of both enzymes POXA1b and POXA1b-Vmh2 (1 U mL^{-1}), in concentrate condition with POXA1b 100 U mL^{-1}, for 2 h at room temperature. Electrodes were then rinsed with 50 mM Tris-HCl buffer solution at pH = 8 and stored at 4 °C.

3. Results and discussion

3.1. Properties of POXA1b and POXA1b-Vmh2 as a MWCNT dispersant

In line with our results on the exfoliation of graphite in the presence of POXA1b-Vmh2 (Sorrentino et al., 2020), the properties of this chimera as a MWCNT surfactant was investigated. Aqueous surfactants such as sodium dodecyl sulfate (SDS) are used to facilitate the preparation of CNT dispersions and their ease of manipulation. However, most surfactants are detrimental to enzyme activity since these molecules are also well-known enzyme denaturants. As shown in Fig. 1, the addition of POXA1b-Vmh2 to a suspension of MWCNTs improved the dispersion stability after sonication for 10 min and centrifugation.

This underlines the surfactant ability of POXA1b-Vmh2 owing to the adhesion properties of the hydrophobin domain towards hydrophobic surface such as MWCNT sidewalls. These results prompted us to study both POXA1b and POXA1b-Vmh2 immobilized at the surface of MWCNT electrodes for bioelectrochemical applications.

3.2. Direct electrochemistry of POXA1b and POXA1b-Vmh2 on pristine MWCNT and anthraquinone-modified MWCNTs

First, the direct electrochemistry of immobilized POXA1b and POXA1b-Vmh2 was studied under Ar and O_2 at pH 5. Fig. 2 shows the direct electrochemistry of POXA1b and POXA1b-Vmh2 on nonmodified and anthraquinone-modified MWCNTs (AQ-MWCNT). AQ-MWCNT were prepared as previously-described (Gentil et al., 2018), by the electrografting of 2-diazoniumanthraquinone tetrafluroroborate in MeCN.

No direct bioelectrocatalytic reduction of O_2 was observed for both POXA1b and POXA1b-Vmh2 on nonmodified MWCNT (curve a, Fig. 2). On AQ-MWCNT, no DET is observed for POXA1b-Vmh2 (data not shown). On the contrary, an irreversible electrocatalytic reduction signal is observed for POXA1b immobilized on AQ-MWCNT (curve b, Fig. 2). Maximum current densities of 150 μA cm^{-2} were observed at 0.1 V *vs.* SCE. Under Ar (black curve b, Fig. 2), a tiny reversible redox system is observed at $E_{1/2} = +0.41$ V vs. SCE or 0.65 V vs. NHE ($\Delta E = 58$ mV), corresponding to an enzyme surface coverage of 5 pmol cm^{-2}. This is the first report of the measurement of the redox potential of POXA1b laccase by direct electrochemistry. It is in good agreement with the redox potential of the T1 copper centre of POXA1b measured at +0.650 V vs. NHE (Garzillo et al., 2001; Pezzella et al., 2017). These results are indicative of a direct wiring of POXA1b on AQ-MWCNT owing to the favourable orientation of the enzyme. This type of behaviour has already been evidenced for *Trametes* laccases (Bourourou et al., 2013; Lalaoui et al, 2015, 2016). However, the fact that no DET is observed for POXA1b-Vmh2 either on nonmodified or AQ-MWCNT electrodes likely indicates that the Vmh2 domain might hinder the electron transfer to the T1 site by adding an insulating domain as well as increased distance between the copper centre and the surface of the electrode. These results prompted us to explore the properties of these two types of modified electrodes towards catechol and dopamine sensing. These biosensors do not rely on direct electron transfer but rather on the efficient immobilization of POXA1b on electrodes either by the chimeric POXA1b-Vmh2 or by the immobilization of POXA1b on AQ-MWCNTs.

3.3. Catechol and dopamine detection by POXA1b and POXA1b-Vmh2 on pristine MWCNT and anthraquinone-modified MWCNTs

Native POXA1b and POXA1b-Vmh2 were compared towards catechol oxidation after their immobilization on MWCNT and AQ-MWCNT electrodes. Catechol biosensing is based on the ability of immobilized laccase to oxidize o-diphenols into quinones in the presence of oxygen. Quinone is subsequently reduced at the electrode poised at a redox potential of E = −0.2 V vs. SCE. The electrogeneration of the phenol derivative induces an amplification cycle of “enzymatic oxidation/

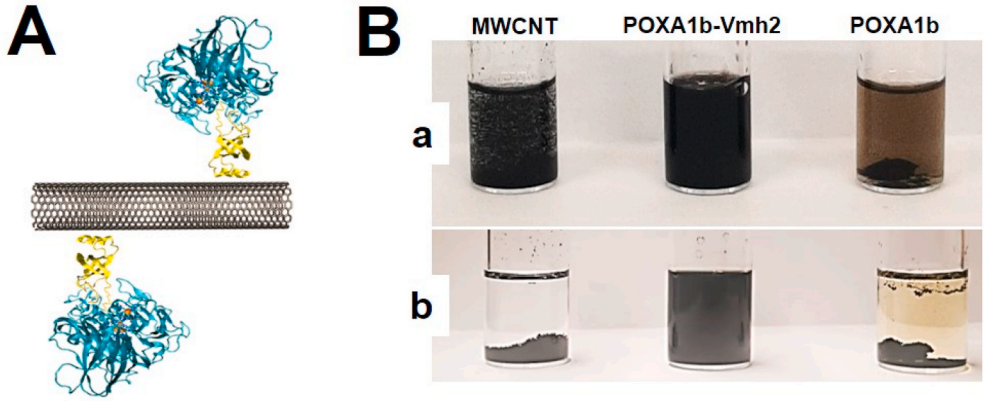

Fig. 1. Panel A: cartoon of POXA1b-Vmh2 bound to a CNT. Panel B: Photograph of the MWCNTs dispersions after ultrasonication and centrifugation in 50% water/ethanol solution (1 mg mL $^{-1}$) before (a) and (b) after 50 days.

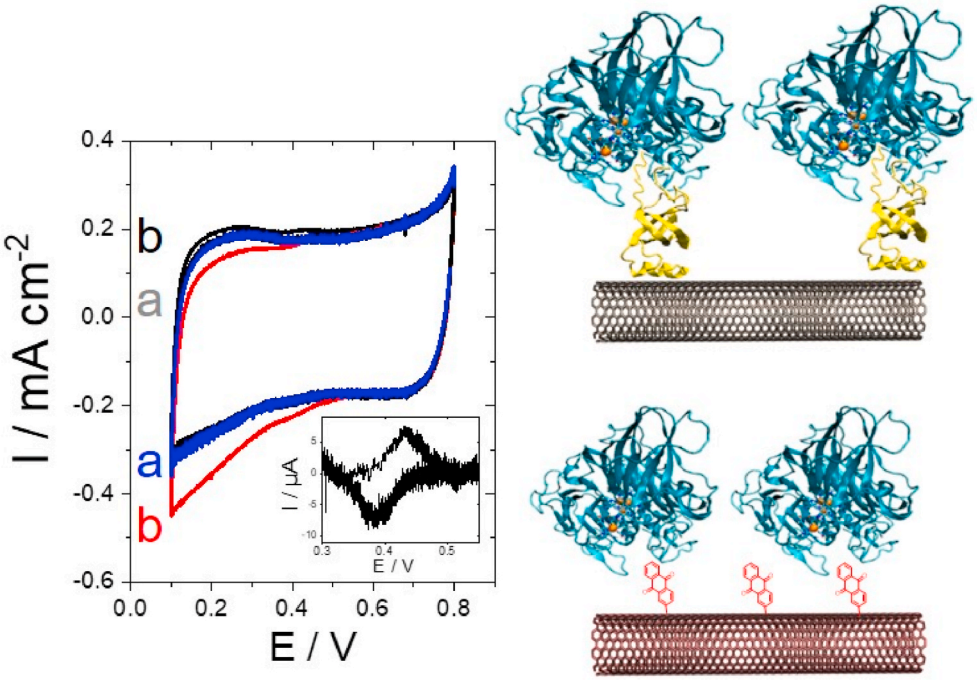

Fig. 2. A schematic representation of POXA1b-Vmh2 and POXA1b immobilized at MWCNT and AQ-MWCNT electrodes, respectively, and corresponding CVs for POXA1b-Vmh2 immobilized at an MWCNT electrode under (a, gray) Ar and (a, blue) O_2 and POXA1b immobilized at an AQ-MWCNT electrode under (b, black) Ar and (b, red) O_2 at pH = 5 (0.1 M phosphate/citrate buffer, v = 10 mV s^{-1}); (inset) Background-subtracted CV of the POXA1b-modified AQ-MWCNT electrode under Ar. (For interpretation of the references to color in this figure legend, the reader is referred to the Web version of this article.)

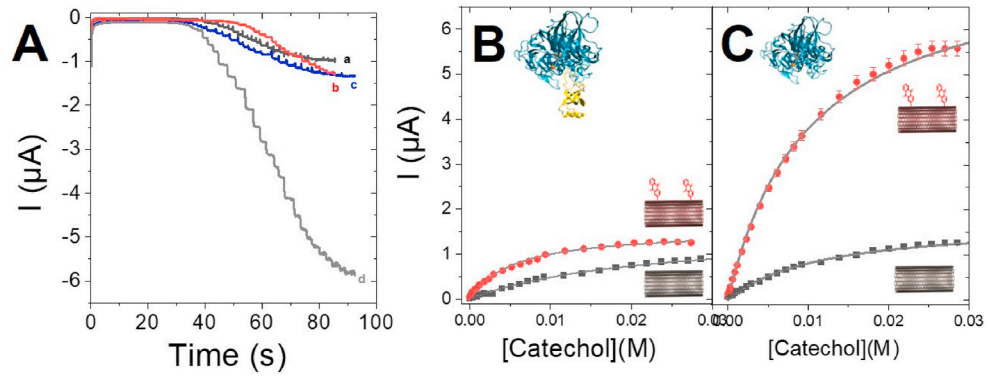

Fig. 3. (A) Chronoamperometry measurements after successive additions of catechol between 0 and 0.03 M for POXA1b-Vmh2 immobilized on (a, black) MWCNT and (b, red) AQ-MWCNT electrodes and POXA1b immobilized on (c, blue) MWCNT and (d, gray) AQ-MWCNT electrodes; Corresponding plot of the catalytic current towards increasing concentrations of catechol for (B) POXA1b-Vmh2 and (C) POXA1b immobilized on MWCNT and AQ-MWCNT electrodes and corresponding fitting curves (gray line) Measurements performed by chronoamperometry at E = −0.2 V vs. SCE, 0.1 M phosphate/citrate buffer, pH 5, 25 °C). Fitting curves were obtained using Origin PRO 9.0 software. (For interpretation of the references to color in this figure legend, the reader is referred to the Web version of this article.)

electrochemical reduction". Amperometric biosensing of catechol is performed by chronoamperometry at different catechol concentrations. Fig. 3 displays chronoamperometry experiments for POXA1b-Vmh2 and POXA1b immobilized (0.02 U for both enzymes) on modified and non-modified MWCNT electrodes.

A typical Michaelis-Menten-type curve was obtained for all electrodes and modelized with the Michaelis-Menten equation. Electrochemical characteristics for all electrodes are displayed in Table 1.

Interestingly, similar curves were obtained for POXA1b and POXA1b-Vmh2 on MWCNT electrodes (black curves from Fig. 3B–C). An increased K_M^{APP} value for POXA1b-Vmh2 might indicate a possible conformation change in the immobilized chimeric enzyme on MWCNTs. This arises from a strong interaction between CNT sidewalls and Vmh2, as confirmed by the high dispersibility of MWCNT in POXA1b-Vmh2 solutions. POXA1b-Vmh2 immobilized on MWCNT electrodes does not show any significant improvement, indicating that the presence of anthraquinone groups at the surface of MWCNT sidewalls does not influence the immobilization or orientation of laccase. On the contrary, POXA1b immobilized on AQ-MWCNT exhibits an almost four-fold increase in maximum current densities (red curve, Fig. 3C). This is in agreement with results observed by direct electrochemistry and the ability of anthraquinone to strongly interact with the substrate pocket of laccase, as already studied by electrochemistry and DFT calculations on *Trametes* laccase (Lalaoui et al., 2016).

3.4. Dopamine and catechol biosensors

Owing to the excellent Michaelis-Menten characteristics of POXA1b laccase immobilized on AQ-MWCNT electrodes, both catechol and dopamine sensors were optimized for this particular configuration. Highly-concentrated POAX1b (2 U, about 100 times more concentrated) was immobilized on anthraquinone-modified MWCNTs to maximize the enzymatic response towards catechol and dopamine. Fig. S1A displays the expected Michaelis-Menten-type dependence for both catechol and dopamine. As expected, high maximum current densities of 25.7 μA were obtained at high catechol concentration. Lower apparent K_M^{APP} values for dopamine (15 mM) were obtained compared to catechol (0.6 mM), owing to the higher affinity of laccase towards catechol.

Fig. 4 shows the presence of two consecutives linear regions for both catechol and dopamine, as has been observed in many enzyme-based phenol sensors(Rodríguez-Delgado et al., 2015).

Two linear regions were identified between 2 and 30 pM and 0.1–800 μM with corresponding sensitivities of 23,600 ($R^2 = 0.972$) and 0.28 ($R^2 = 0.992$) mA L $mmol^{-1}$ cm^{-2} for catechol (Fig. 4A and B), respectively. For dopamine, two linear regions were identified between 0.015-90 μM and 30-30 μM with corresponding sensitivities of 0.053 ($R^2 = 0.975$) and 0.033 ($R^2 = 0.999$) mA L $mmol^{-1}$ cm^{-2} (Fig. 4C and D), respectively. Excellent biosensing characteristics make this biosensor one of the most sensitive biosensors based on laccase for both catechol and dopamine. Furthermore, no chronoamperometric response was observed during biosensing experiments after the addition of two interferents, 50 μM ascorbic acid and 50 μM uric acid. It is noteworthy that these biosensing performances are several orders of magnitude higher as compared to our previously-developed hydrophobin-fused chimera Vmh2-POXA1b immobilized on few-layer graphene.(Sorrentino et al., 2020). This likely accounts for the nonoptimized functionalization of graphene nanosheets with chimera laccase and the superior conductivity of MWCNT films as compared to biofunctionalized graphene. Table 2 and summarizes previously-developed biosensors based on tyrosinases and laccases for catechol and dopamine. The POXA1b-modifed AQ-MWCNT electrode outperforms most laccase-based biosensors for catechol and provides higher limit-of-detection compared to nanostructured biosensors based on both laccase or tyrosinase. For dopamine sensing, AQ-MWCNT-supported POXA1b approaches the best performances of other types of laccase and tyrosinase biosensors.

Table 1
Simulated Electrochemical characteristics obtained from the plot of the catalytic current towards increasing concentrations of catechol in Fig. 3B–C.

		K_M^{APP} (mol L^{-1})	I_{max} (μA)	R^2
POXA1b	MWCNT	0.010 (±0.001)	1.74 (±0.10)	0.998
	AQ-MWCNT	0.011 (±0.001)	7.62 (±0.05)	0.992
POXA1b-Vmh2	MWCNT	0.022 (±0.002)	1.54 (+/0.04)	0.997
	AQ-MWCNT	0.007 (±0.001)	1.55 (±0.05)	0.991

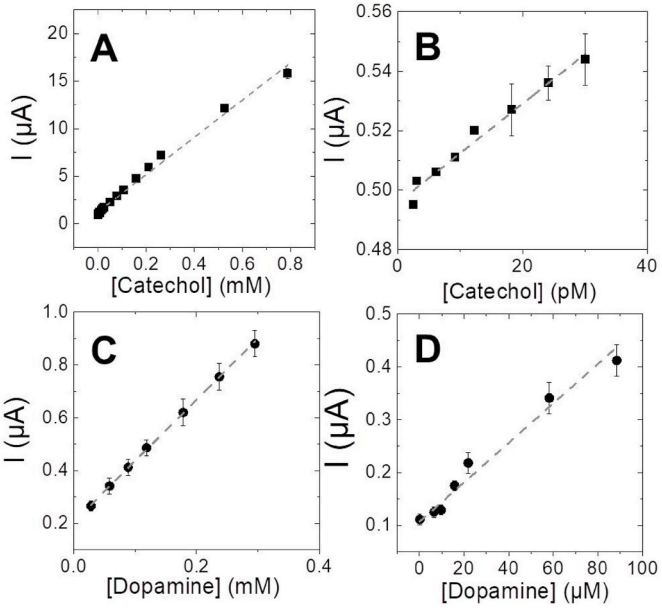

Fig. 4. Linear sections of the plots for catalytic current towards catechol (A, B) and dopamine (C, D) concentration.

Furthermore, the stability of this sensor was tested at high salinity from 0 to 0.5 M NaCl to estimate its ability to operate in seawater samples. It is well known that the extensively studied *Trametes* laccases are highly sensitive towards chloride inhibition(Le Goff et al., 2015; Mano and de Poulpiquet, 2017; Vaz-Dominguez et al., 2008). Here, owing to the exceptional stability of POXA1b at high chloride concentration, the nanostructured biosensor retains 30% of its initial activity at 0.5 M NaCl (Fig. S1B).

4. Conclusion

In this work, we investigated the electrochemical characteristics of POXA1b and its hydrophobin-based fused chimera on functionalized MWCNTs, either for direct electroenzymatic reduction of O_2 or indirect electrochemical biosensing of catechol and dopamine. While POXA1b-Vmh2 gives access to stable CNT dispersions in water/ethanol mixtures, its Vmh2 increases the distance between the electrode surface and the enzyme active site. This prevents its use in direct electrochemistry. On the contrary, anthraquinone-modified MWCNTs are able to efficiently immobilize POXA1b laccase, showing, for the first time for this particular laccase, direct electrocatalytic reduction of O_2. The fact that anthraquinone greatly improves POXA1b immobilization, and not for POXA1b-Vmh2, is indicative of the fact that the Vmh2 domain competes with the hydrophobic patch at the surface of the native POXA1b for the efficient immobilization of the enzyme. The combination of AQ-MWCNT with POXA1b gives access to a highly sensitive biosensor for catechol and dopamine, leading to unprecedented picomolar detection for catechol and micromolar detection of dopamine, accompanied with respective sensitivities of 23,600 mA L $mmol^{-1}$ cm^{-2} and 0.053 mA L $mmol^{-1}$. This work provides new insights into the nature of the interactions of POXA1b and its chimera at the surface of MWCNTs. While

Table 2
Electrochemical characteristics of biosensors based on tyrosinases and laccases for catechol and dopamine electrochemical biosensing.

Catechol biosensor	Enzyme	Linear range	Sensitivity (mA L mmol-1 cm^{-2})	References
POxA1b/AQ-MWCNT	POXA1b	2–30 pM 0.1–800 μM	23,600 0.28	This work
POxA1b-vmh2/graphene	POXA1b	20–1000 μM	0.00027	Sorrentino et al. (2020)
Graphene/cellulose microfiber	*Trametes versicolor*	0.085–210 μM	0.0009	Palanisamy et al. (2017)
reduced graphene oxide/chitosan	*Rhus vernicifera* laccase	7–700 μM	0.00011	Zhou et al. (2013)
tungsten disulfide nanotubes	Tyrosinase	0.6–70 μM	0.151	Palomar et al. (2020)
CNT + CaCO3 nanoparticles	Tyrosinase	1–8 μM	35.7	Bujduveanu et al. (2013)
Gold nanoparticle + screen printed carbon electrode	tyrosinase	1.1–80 μM	49	Karim et al. (2014)
screen-printed carbon electrode	horseradish peroxidase/ tyrosinase	0.120–43 μM	0.00185	Chang et al. (2002)
circular glassy carbon electrode	Tyrosinase	0–0.631 μM	0.213	Adamski et al. (2010)
CPE-Tyr-Inc (incorporated lyophilized Tyr)	Tyrosinase	2.5–17.5 μM	1400	Nadifiyine et al. (2013)
CPE-Tyr (graphite)		5–85 μM	1640	
CBPE-Tyr (carbon black		0.013–150 μM	1720	
single-wall carbon nanotubes (SWCNTs) and polyaniline (PANI)	Tyrosinase	0.25–92 μM	0.144	Wang et al. (2013)
Tyr-AuNPs-DHP/GCE	Tyrosinase	2.5–95 μM	0.115	Campanhã Vicentini et al. (2016)
GCE/hybrid/enzyme/membrane	Tyrosinase or laccase	0–300 μM	310	Vlamidis et al. (2017)
Dopamine biosensor				
POxA1b/AQ-MWCNT	POXA1b	0.01–90 μM 30–300 μM	0.053 0.033	This work
POxA1b-vmh2/graphene	POXA1b	20–250 μM	0.000016	Sorrentino et al. (2020)
Si/MWCNT/Screen-printed electrode	*Trametes versicolor laccase*	1.3–85.5 μM	2.787	Li et al. (2012)
3-mercaptopropionic acid-modified gold electrode	*Agaricus bisporus* laccase	0.5–13 μM 47–430 μM	1.95 0.92	Shervedani and Amini (2012)
tungsten disulfide nanotubes	Commercial Tyrosinase	0.5–10 μM 10–40 μM	0.0087 0.0048	Palomar et al. (2020)
CNT + CaCO3 nanoparticles	Commercial Tyrosinase	0.015–30 μM	3.57	Bujduveanu et al. (2013)
CNT/glutaraldehyde/PEDOT on gold microelectrode array	Commercial Tyrosinase	100–500 μM	1120	Lete et al. (2015)
SWNT/Ppy	Commercial tyrosinase	5–50 μM	0.467	Min and Yoo (2009)

the Vmh2 domain provides a soft functionalization route for immobilization of redox enzymes, the fusion protein still needs more developments that take into account the nature of the interactions with the corresponding surface as well as the accessibility of both the substrate and electrons, especially for bioelectrocatalytic applications. Owing to the wide spectrum of phenolic substrates of laccase and the stability of POXA1b in harsh conditions, this work paves the way for the use of this particular enzyme for many types of laccase-based electrochemical biosensors, while also providing future directions for the engineering of new chimera redox proteins.

CRediT authorship contribution statement

Ilaria Sorrentino: Experiments. **Ilaria Stanzione:** Experiments. **Alessandra Piscitelli:** Writing – review & editing, Supervision, Project administration, Funding acquisition. **Paola Giardina:** Writing – review & editing, Supervision, Project administration, Funding acquisition. **Alan Le Goff:** Writing – review & editing, Supervision, Project administration, Funding acquisition.

Declaration of competing interest

The authors declare that they have no known competing financial interests or personal relationships that could have appeared to influence the work reported in this paper.

Acknowledgements

This project is funded by the Italian Education, University and Research Ministry (MIUR) and the French National Research Agency (ANR), and co-funded by European Union's Horizon 2020 research and innovation program under the framework of ERA-NET Cofund MarTERA (Maritime and Marine Technologies for a new Era), FLAshMoB, Functional Amyloid chimera for Marine Biosensing (ID: 172). This work was also supported by the Agence Nationale de la Recherche through the LabEx ARCANE programme (ANR-11-LABX-0003-01) and the Graduate School on Chemistry, Biology and Health of Univ Grenoble Alpes CBH-EUR-GS (ANR-17-EURE-0003). The authors acknowledge support from the plateforme de Chimie NanoBio ICMG FR 2607 (PCN-ICMG).

Appendix A. Supplementary data

Supplementary data to this article can be found online at https://doi.org/10.1016/j.biosx.2021.100074.

References

Adamski, J., Nowak, P., Kochana, J., 2010. Electrochim. Acta 55, 2363–2367. https://doi.org/10.1016/j.electacta.2009.11.099.
Askolin, S., Linder, M., Scholtmeijer, K., Tenkanen, M., Penttilä, M., de Vocht, M.L., Wösten, H.A.B., 2006. Biomacromolecules 7, 1295–1301. https://doi.org/10.1021/bm050676s.
Bourourou, M., Elouarzaki, K., Lalaoui, N., Agnès, C., Le Goff, A., Holzinger, M., Maaref, A., Cosnier, S., 2013. Chem. Eur J. 19, 9371–9375. https://doi.org/10.1002/chem.201301043.
Bujduveanu, M.-R., Yao, W., LeGoff, A., Gorgy, K., Shan, D., Diao, G.-W., Ungureanu, E.-M., Cosnier, S., 2013. Electroanalysis 25, 613–619. https://doi.org/10.1002/elan.201200245.
Campanhã Vicentini, F., Garcia, L.L.C., Figueiredo-Filho, L.C.S., Janegitz, B.C., Fatibello-Filho, O., 2016. Enzym. Microb. Technol. 84, 17–23. https://doi.org/10.1016/j.enzmictec.2015.12.004.
Chang, S.C., Rawson, K., McNeil, C.J., 2002. Biosens. Bioelectron. 17, 1015–1023. https://doi.org/10.1016/S0956-5663(02)00094-5.

De Stefano, L., Rea, I., Armenante, A., Giardina, P., Giocondo, M., Rendina, I., 2007. Langmuir 23, 7920–7922. https://doi.org/10.1021/la701189b.
De Stefano, L., Rea, I., De Tommasi, E., Rendina, I., Rotiroti, L., Giocondo, M., Longobardi, S., Armenante, A., Giardina, P., 2009. Eur. Phys. J. E 30, 181. https://doi.org/10.1140/epje/i2009-10481-y.
Garzillo, A.M., Colao, M.C., Buonocore, V., Oliva, R., Falcigno, L., Saviano, M., Santoro, A.M., Zappala, R., Bonomo, R.P., Bianco, C., Giardina, P., Palmieri, G., Sannia, G., 2001. J. Protein Chem. 20, 191–201. https://doi.org/10.1023/A:1010954812955.
Gentil, S., Che Mansor, S.M., Jamet, H., Cosnier, S., Cavazza, C., Le Goff, A., 2018. ACS catal. https://doi.org/10.1021/acscatal.8b00708, 3957-3964.
Gravagnuolo, A.M., Morales-Narváez, E., Longobardi, S., da Silva, E.T., Giardina, P., Merkoçi, A., 2015. Adv. Funct. Mater. 25, 2771–2779. https://doi.org/10.1002/adfm.201500016.
Holzinger, M., Le Goff, A., Cosnier, S., 2017. Sensors 17, 1010. https://doi.org/10.3390/s17051010.
Karim, MdN., Lee, J.E., Lee, H.J., 2014. Biosens. Bioelectron. 61, 147–151. https://doi.org/10.1016/j.bios.2014.05.011.
Lalaoui, N., David, R., Jamet, H., Holzinger, M., Le Goff, A., Cosnier, S., 2016. ACS Catal. 6, 4259–4264. https://doi.org/10.1021/acscatal.6b00797.
Lalaoui, N., LeGoff, A., Holzinger, M., Mermoux, M., Cosnier, S., 2015. Chem. Eur J. 21, 3198–3201. https://doi.org/10.1002/chem.201405557.
Le Goff, A., Holzinger, M., 2018. Sustainable Energy Fuels 2, 2555–2566. https://doi.org/10.1039/C8SE00374B.
Le Goff, A., Holzinger, M., Cosnier, S., 2015. Cell. Mol. Life Sci. 72, 941–952. https://doi.org/10.1007/s00018-014-1828-4.
Lete, C., Lupu, S., Lakard, B., Hihn, J.-Y., del Campo, F.J., 2015. J. Electroanal. Chem. 744, 53–61. https://doi.org/10.1016/j.jelechem.2015.03.005.
Li, Y., Zhang, L., Li, M., Pan, Z., Li, D., 2012. Chem. Cent. J. 6, 103. https://doi.org/10.1186/1752-153X-6-103.
Longobardi, S., Gravagnuolo, A.M., Funari, R., Della Ventura, B., Pane, F., Galano, E., Amoresano, A., Marino, G., Giardina, P., 2015. Anal. Bioanal. Chem. 407, 487–496. https://doi.org/10.1007/s00216-014-8309-3.
Mano, N., de Poulpiquet, A., 2017. O2 Chem. Rev. 118, 2392–2468. https://doi.org/10.1021/acs.chemrev.7b00220.
Min, K., Yoo, Y.J., 2009. Talanta 80, 1007–1011. https://doi.org/10.1016/j.talanta.2009.08.032.
Nadifiyine, S., Haddam, M., Mandli, J., Chadel, S., Blanchard, C.C., Marty, J.L., Amine, A., 2013. Anal. Lett. 46, 2705–2726. https://doi.org/10.1080/00032719.2013.811679.
Palanisamy, S., Ramaraj, S.K., Chen, S.-M., Yang, T.C.K., Yi-Fan, P., Chen, T.-W., Velusamy, V., Selvam, S., 2017. Sci. Rep. 7, 1–12. https://doi.org/10.1038/srep41214.
Palomar, Q., Gondran, C., Lellouche, J.-P., Cosnier, S., Holzinger, M., 2020. J. Mater. Chem. B 8, 3566–3573. https://doi.org/10.1039/C9TB01926J.
Pezzella, C., Giacobelli, V.G., Lettera, V., Olivieri, G., Cicatiello, P., Sannia, G., Piscitelli, A., 2017. J. Biotechnol. 259, 175–181. https://doi.org/10.1016/j.jbiotec.2017.07.022.
Pezzella, C., Guarino, L., Piscitelli, A., 2015. Cell. Mol. Life Sci. 72, 923–940. https://doi.org/10.1007/s00018-014-1823-9.
Portaccio, M., Gravagnuolo, A.M., Longobardi, S., Giardina, P., Rea, I., De Stefano, L., Cammarota, M., Lepore, M., 2015. Appl. Surf. Sci. 351, 673–680. https://doi.org/10.1016/j.apsusc.2015.05.182.
Rodríguez-Delgado, M.M., Alemán-Nava, G.S., Rodríguez-Delgado, J.M., Dieck-Assad, G., Martínez-Chapa, S.O., Barceló, D., Parra, R., 2015. Trac. Trends Anal. Chem. 74, 21–45. https://doi.org/10.1016/j.trac.2015.05.008.
Shervedani, R.K., Amini, A., 2012. Bioelectrochemistry 84, 25–31. https://doi.org/10.1016/j.bioelechem.2011.10.004.
Sorrentino, I., Gentil, S., Nedellec, Y., Cosnier, S., Piscitelli, A., Giardina, P., LeGoff, A., 2019a. ChemElectroChem 5, 1–6. https://doi.org/10.1002/celc.201801264.
Sorrentino, I., Giardina, P., Piscitelli, A., 2019b. Appl. Microbiol. Biotechnol. 103, 3061–3071. https://doi.org/10.1007/s00253-019-09678-2.
Sorrentino, I., Stanzione, I., Nedellec, Y., Piscitelli, A., Giardina, P., Le Goff, A., 2020. Int. J. Mol. Sci. 21, 3741. https://doi.org/10.3390/ijms21113741.
Sosna, M., Stoica, L., Wright, E., Kilburn, J.D., Schuhmann, W., Bartlett, P.N., 2012. Phys. Chem. Chem. Phys. 14, 11882.
Sotiropoulou, S., Gavalas, V., Vamvakaki, V., Chaniotakis, N.A., 2003. Biosens. Bioelectron. 18, 211–215. https://doi.org/10.1016/S0956-5663(02)00183-5.
Valentini, F., Carbone, M., Palleschi, G., 2013. Anal. Bioanal. Chem. 405, 451–465. https://doi.org/10.1007/s00216-012-6351-6.
Vaz-Dominguez, C., Campuzano, S., Rüdiger, O., Pita, M., Gorbacheva, M., Shleev, S., Fernandez, V.M., De Lacey, A.L., 2008. Laccase electrode for direct electrocatalytic reduction of O_2 to H_2O with high-operational stability and resistance to chloride inhibition. Biosens. Bioelectron. 24, 531–537. https://doi.org/10.1016/j.bios.2008.05.002.
Vlamidis, Y., Gualandi, I., Tonelli, D., 2017. J. Electroanal. Chem. 799, 285–292. https://doi.org/10.1016/j.jelechem.2017.06.012.
Wang, B., Zheng, J., He, Y., Sheng, Q., 2013. Sensor. Actuator. B Chem. 186, 417–422. https://doi.org/10.1016/j.snb.2013.06.016.
Wang, Z., Lienemann, M., Qiau, M., Linder, M.B., 2010. Langmuir 26, 8491–8496. https://doi.org/10.1021/la101240e.
White, S.H., 2004. Protein Sci. 13, 1948–1949. https://doi.org/10.1110/ps.04712004.
Zhou, X.-H., Liu, L.-H., Bai, X., Shi, H.-C., 2013. Sensor. Actuator. B Chem. 181, 661–667. https://doi.org/10.1016/j.snb.2013.02.021.